

# Nanomechanics of vimentin intermediate filament networks

Sarah Köster,<sup>ab</sup> Yi-Chia Lin,<sup>b</sup> Harald Herrmann<sup>c</sup> and David A. Weitz<sup>\*b</sup>

Received 6th January 2010, Accepted 25th February 2010

First published as an Advance Article on the web 11th March 2010

DOI: 10.1039/c000113a

Intermediate filaments are one of three classes of fibrous proteins in the cytoskeleton of eukaryotes, the others being actin filaments and microtubules. The dense filamentous networks and bundles provide important mechanical stability for the cell. Here we directly measure both the structure and mechanical properties of an *in vitro* model system for intermediate filaments reconstituted from purified vimentin protein at 1 mg mL<sup>-1</sup>. We show that the mesh size is on the order of 1 μm, a value that is preserved upon addition of divalent ions. These ions act as effective cross-linkers, further stiffening the network.

## Introduction

The physical properties and mechanics of animal cells are controlled mainly by three types of filament systems: actin filaments, microtubules and intermediate filaments (IFs). In addition, numerous associated binding proteins are essential, particularly for the actin networks. Moreover, both actin filaments and microtubules serve as tracks for molecular motors, which help to determine the structure and mechanical properties of cells. Actins and tubulins, the constituents of actin filaments and microtubules, respectively, are globular proteins, and they are highly conserved in eukaryotic cells. In contrast, IF proteins are fibrous polypeptides coded for by a large gene family, whose members exhibit relatively little primary sequence identity but a distinctly conserved structural plan. Notably, even within the same organism different cell types express different types and amounts of the respective proteins.<sup>1</sup> One of the most abundant IF proteins is vimentin, which is found in cells of mesenchymal origin such as fibroblasts, endothelial cells and smooth muscle cells. In these cells, vimentin forms cytoplasmic networks that are believed to contribute to the mechanical stability of the cell.<sup>2</sup> The physical attributes of cells are influenced by numerous components and parameters; thus investigation of purified *in vitro* networks is a valuable tool for a better understanding of the material properties of biopolymer networks in living cells.<sup>3–6</sup>

Bulk studies employing tensile tests<sup>7</sup> and bulk rheology<sup>8</sup> show a Young's modulus of 7 MPa. The network stiffness increases considerably upon addition of divalent ions such as magnesium (Mg<sup>2+</sup>), calcium (Ca<sup>2+</sup>) and zinc (Zn<sup>2+</sup>); similar behavior is found upon addition of trivalent and tetravalent ions. Interestingly, these rheological studies suggest that multivalent ions act as effective cross-linkers by analogy to actin-binding proteins (ABPs) in actin networks.<sup>8</sup>

The persistence length and the Young's modulus of vimentin filaments and the mesh size of vimentin networks have been

determined from bulk rheological measurements by fitting the data to a model that assumes an entropic origin of the elasticity. However, the microscale structure may sensitively influence local mechanical properties and it is therefore important to directly probe both structure and rheology on the length scale of the expected mesh size. Unfortunately, a direct measurement of the microstructure of vimentin networks as well as its dependence on ion concentration and cross-linking is still largely missing. Such measurements would complement the bulk studies and confirm the validity of their interpretation in determining the micro-mechanical properties of biopolymer networks. Moreover investigations on all levels would provide a complete picture of the structure, dynamics, and mechanics of cytoskeletal protein networks.

Here we directly probe the mesh size and heterogeneity of reconstituted vimentin networks by monitoring the thermal motion of microspheres with diameters on the order of the mesh size. In addition, we use larger probe particles to measure the rheological properties, using microrheology. Our results are in very good agreement with recent bulk rheology measurements. Furthermore, our data provide direct evidence that Mg<sup>2+</sup> ions at low concentration act as effective cross-linkers in the network, with little change in network structure. Moreover, the measured mesh size is in good agreement with theoretical expectations based on a geometric estimate of the networks structure and bulk measurements of the modulus.

## Results and discussion

Measuring the thermally induced motion of probe particles within the IF network provides two different classes of information, probing both the structure and the mechanics of the network. Depending on the ratio of mesh size of the protein network and the diameter of the microspheres, the microspheres can either move within the network or are immobilized and trapped. The particles that move within the network provide a measure of the mesh size and heterogeneity of the network structure, while particles that remain locally trapped provide a measure of the rheological properties of the network. We therefore choose microspheres whose sizes span the expected range of the mesh size. Assuming a simple "cubic" model for the network, the mesh size,  $\xi$ , in micrometres can be calculated<sup>9</sup>

<sup>a</sup>Courant Research Centre Nano-Spectroscopy and X-Ray Imaging, University of Göttingen, Friedrich-Hund-Platz 1, 37077 Göttingen, Germany

<sup>b</sup>Department of Physics and School of Engineering and Applied Sciences, Harvard University, Cambridge, MA, 02138, USA. E-mail: weitz@seas.harvard.edu

<sup>c</sup>German Cancer Research Center (DKFZ), B065, Im Neuenheimer Feld 280, 69120 Heidelberg, Germany

from the molecular weight ( $M_w = 53$  kDa), the concentration ( $c = 1$  mg mL<sup>-1</sup>) of vimentin, and the number of (32) monomers per unit length filament (ULF,  $\sim 45$  nm):

$$\xi = 0.45 \times c^{-1/2} = 0.45 \mu\text{m} \quad (1)$$

We therefore record  $x$ - $y$  tracks of individual microspheres with diameters  $d = 0.5$ , 1, and 2  $\mu\text{m}$ , and show representative examples in Fig. 1. The first set of experiments is performed with pure vimentin networks and no additional ions (Fig. 1a). In this case, we find that the largest microspheres ( $d = 2$   $\mu\text{m}$ , black) are indeed trapped in the network and can only move within a restricted microenvironment. By contrast, the smaller microspheres ( $d = 1$   $\mu\text{m}$ , red, and  $d = 0.5$   $\mu\text{m}$ , blue) show a strikingly different behavior: some of them are still constrained and move within the confining mesh of the network (right hand side of Fig. 1a). Others, however, move in one distinct microenvironment but eventually jump to another, where they continue their motion. From this behavior we conclude that the microspheres are small enough to slip through the entangled filaments that form the network and probe separate microenvironments. Similar behavior is observed for entangled actin networks.<sup>10</sup>

To further study the behavior of the microspheres in entangled vimentin networks, we plot the averaged mean-squared

displacements (MSDs) for each set of microspheres in Fig. 1c. Each curve shown represents an average of up to thousands of individual datasets, where several trajectories may belong to each microsphere in the field of view. Only tracks that are at least ten steps long are included in the averaging. We used two different frequencies to record the data, 1000 Hz and 20 Hz, and calculated the MSDs for each set. The data match together quite well without any scaling, as shown in Fig. 1. The dashed and dotted lines in Fig. 1c show the one-dimensional MSDs for microspheres in buffer, performed as a control experiment. From the slope of the data from these control experiments the diffusion constant  $D$  can be determined:

$$\Delta x(\tau)^2 = 2D\tau \quad (2)$$

Here,  $\tau$  is the lag time between two data points and  $x$  is the corresponding particle position. We find the values for  $D$  to be consistent with the Stokes–Einstein equation assuming the viscosity of the buffer to be  $\eta_{\text{water}} = 1$  mPa s:

$$\eta = \frac{k_B T}{3\pi D d} \quad (3)$$

where  $d$  is the diameter of the sphere,  $k_B$  is Boltzman's constant and  $T$  is the temperature. The microscopy images of the 2  $\mu\text{m}$  diameter beads are not as clear as those of the smaller beads, making the particle tracking less precise and leading to an increased noise floor. This effect is clearly seen in the data for the 2  $\mu\text{m}$  diameter beads in buffer at lowest frequencies, where the data saturate at about  $10^{-2}$   $\mu\text{m}^2$ , as shown by the dotted black line in Fig. 1c.

The data for the microspheres in aqueous buffer exhibit diffusive Brownian motion as described by eqn (2). By contrast, the MSDs of microspheres in entangled vimentin networks (solid lines and open circles in Fig. 1c) exhibit subdiffusive behavior:

$$\Delta x(\tau)^2 = 2D\tau^\beta \quad (4)$$

with  $\beta < 1$ . In the case of entangled actin networks such a diffusive exponent less than one can result from the power-law distribution of times between the jumps of the microspheres between different microenvironments.<sup>10</sup> Given the apparent jumps in the individual tracks (Fig. 1a) it is very likely that the subdiffusive MSDs shown here result from a similar effect.

For actin networks, numerous specific cross-linkers, or actin-binding proteins (ABPs) exist and their influence on network mechanics has been studied extensively. By contrast, only few such cross-linkers have been identified for IFs. It thus remains an open question how cellular IF networks can provide such remarkable strength and stability. Recently, results of bulk rheology studies have suggested that divalent ions such as  $\text{Mg}^{2+}$  act as effective cross-linkers in networks of vimentin and neurofilaments.<sup>8</sup> To directly test this finding on a microscopic level, we perform a set of experiments with the same microsphere sizes but with 2 mM  $\text{MgCl}_2$  added to the protein solution during assembly. In this case, the molar ratio of  $\text{Mg}^{2+}$  ions and vimentin monomers is  $R = c_{\text{Mg}}/c = 105$ . This value sets the distance between cross-links. By analogy to Fig. 1a, we show representative  $y(x)$  tracks in vimentin networks with  $\text{Mg}^{2+}$  added in Fig. 1b. The concentration of  $\text{Mg}^{2+}$  used here is much lower than

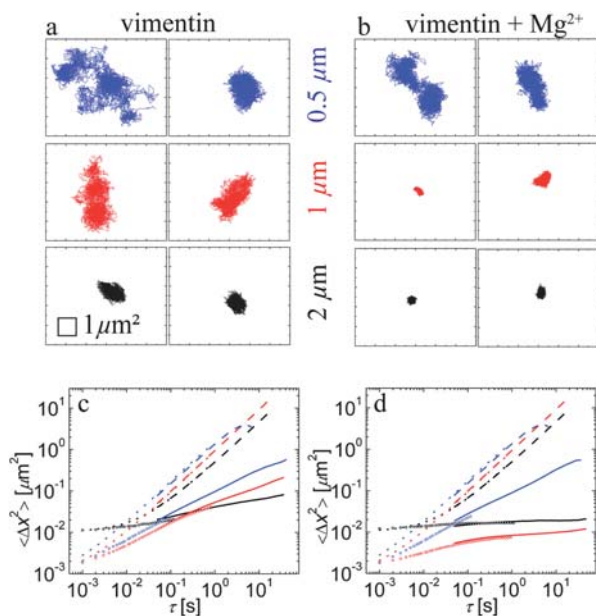


**Fig. 1** (a) Individual  $y$ - $x$  tracks for microspheres in vimentin, with diameters of 0.5  $\mu\text{m}$  (top, blue), 1  $\mu\text{m}$  (center, red), 2  $\mu\text{m}$  (bottom, black). The smaller microspheres “jump” between different microenvironments while the largest microspheres are caged in the network. (b) Individual tracks for microspheres in vimentin with 2 mM  $\text{Mg}^{2+}$  (color code as in (a)). Only the smallest microspheres show considerable movement in the network while the 1 and 2  $\mu\text{m}$  diameter microspheres are caged and move very little. (c) Mean-squared displacement of microspheres (color code as in (a)) in buffer (dashed and dotted lines) and in entangled vimentin (1 mg mL<sup>-1</sup> networks (solid lines and open circles)). In vimentin networks the microspheres show sub-diffusive behavior. (d) Mean-squared displacement of microspheres color code as in (a) in buffer (dashed and dotted lines) and in cross-linked vimentin (1 mg mL<sup>-1</sup> protein with 2 mM  $\text{Mg}^{2+}$ ,  $R = 105$ ) networks (solid lines and open circles).

concentrations commonly used for counter ion condensation of negatively charged biopolymers. For example, actin shows distinct bundling upon addition of about 80 mM  $\text{Ca}^{2+}$ .<sup>11</sup> The smallest microspheres, with diameter 0.5  $\mu\text{m}$ , show the same movement whether or not there is  $\text{Mg}^{2+}$  present, including the jumps between microenvironments. This is also apparent in the corresponding MSD (blue solid line and open circles in Fig. 1d). By contrast, however, the larger microspheres (1 and 2  $\mu\text{m}$  diameter) do not show any jumps between microenvironments and appear to be more highly trapped and thus confined within the networks with added  $\text{Mg}^{2+}$  than in entangled networks as it is apparent in the much smaller volumes they explore during the total time they are recorded. This is reflected by the plateau reached by their MSDs for larger  $\tau$ , shown in Fig. 1d. From these plateau values of the 1 and 2  $\mu\text{m}$  diameter beads, the elastic modulus can be estimated:

$$G' \approx \frac{2k_{\text{B}}T}{d\langle\Delta x^2\rangle} \quad (5)$$

We obtain a value of about 0.7 Pa from the 1  $\mu\text{m}$  diameter beads, which is in good agreement with the results from bulk rheology measurements. The 2  $\mu\text{m}$  diameter beads are more constrained by the network; however, the data for them are obscured by the noise floor.

Smaller beads are not suitable for measuring the rheology of the vimentin network, since they are not trapped by the mesh of the network and therefore do not probe the elastic properties of the material. The same holds true for the beads which are embedded in entangled vimentin networks and small enough to slip through the filaments. Instead, we can estimate the mesh size of the network from the motion of these particles. In Fig. 1d we see that in the networks with added  $\text{Mg}^{2+}$  the 0.5  $\mu\text{m}$  beads are not trapped in the mesh work as they do not reach a plateau level even for large lag times  $\tau$ . In the networks without  $\text{Mg}^{2+}$  (see Fig. 1c) only the largest beads are weakly trapped and we can use the MSD curves of the 0.5 and 1  $\mu\text{m}$  diameter beads to estimate the mesh size. By adding the square root of the MSD to the microsphere diameter we obtain values between 1.2 and 1.5  $\mu\text{m}$ ; these values very likely represent upper bounds as the beads are most probably trapped in the largest pore spaces. Thus, given the uncertainty of these measurements, these estimates are in reasonable agreement with the calculated value of 0.45  $\mu\text{m}$  and the value of 0.175  $\mu\text{m}$  to 0.6  $\mu\text{m}$  determined from bulk rheology measurements.<sup>8,12</sup>

Bulk rheology data<sup>8</sup> suggest that the elasticity of IF networks is very similar to that of actin networks, with the  $\text{Mg}^{2+}$  ions acting in the same way as do rigid cross-linking actin-binding proteins such as scruin.<sup>13</sup> Such networks are well described by an entropic spring model which assumes that thermal fluctuations of individual filaments are pulled out upon application of an external shear.<sup>8</sup>

An important assumption of this model is that the network deformation is affine. To confirm this, we probe microscopic deformation by directly imaging the microscale strain field of sheared networks and measure the resulting degree of non-affinity. We form a network in a shear cell, apply strain, and then image fluorescent, 2  $\mu\text{m}$  diameter particles embedded in the network. These particles are large enough to ensure that they are trapped within the network, and allow us to probe the

non-affinity of the network at length scales down to roughly their size. We probe networks with vimentin concentrations of 3 and 4  $\text{mg mL}^{-1}$  without  $\text{Mg}^{2+}$  and with added  $\text{Mg}^{2+}$  at a molar ratio of  $R = 134$ . We use a higher vimentin concentration for these experiments than for the microrheology study, because the particles are not completely trapped in 1  $\text{mg mL}^{-1}$  networks as determined from the data shown in Fig. 1. By increasing the vimentin concentration we ensure that the microspheres are completely trapped; thus, the deviation of the actual particle position from that expected for an affine deformation is larger than the noise level. We track positions of particles  $y$  at height  $z$  at each applied strain  $\gamma$ . The particle displacement in the shear direction  $\Delta y$  is linear with height  $z$  (data not shown). The degree of non-affinity is defined as  $N(r) = \langle r^2 \Delta\theta^2 \rangle / \gamma^2$ , where we average over all pairs of particles separated by  $r$ ,  $\gamma$  is the applied strain and  $r\Delta\theta$  corresponds to the deviation of the separation from the strictly affine motion.<sup>14,15</sup> We find that the value of  $N(r, \gamma)$  ranges between  $10^{-2}$  and 10 which is similar to values observed for actin networks cross-linked by scruin; this suggests that the strain in vimentin networks is predominantly affine at these concentrations, just as it is for actin networks.<sup>14</sup> In addition, the overall behavior is similar to that observed for actin networks cross-linked with scruin. In both cases we observe a weak increase of  $N$  with  $r$ , as seen in Fig. 2a for the vimentin networks. The increase is described by  $N(r) = r^\alpha$ ,  $\alpha < 2$ , again by analogy with the actin data this suggests that the network is rather flexible.<sup>14</sup> Moreover,  $N$  is nearly independent of the applied strain at a fixed  $r$ , as seen in Fig. 2b. Here, this is expected for small strains,<sup>15</sup> since the deviation of each particle from its ideal displacement under a uniform shear is itself proportional to the strain. Interestingly, we observe such strain-independence of  $N(r)$  for strains up to  $\sim 1.3$ .

We observe that the network deformation becomes more affine at higher  $c$  and slightly more affine at higher  $R$ , as indicated by the decrease in  $N$ ; this is analogous to the behavior of actin networks cross-linked by scruin.<sup>14</sup> These observations add further evidence to support our assumption that the elasticity of vimentin networks is due to affine stretching of the filaments.

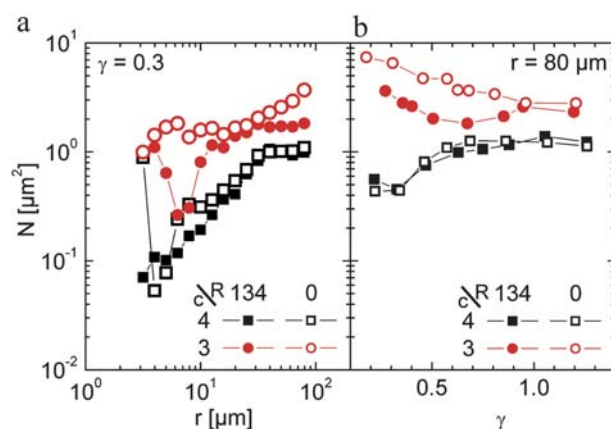


**Fig. 2** Shear deformation of vimentin networks is affine. (a) Degree of non-affinity,  $N$ , plotted against the distance  $r$  between the particles at a fixed strain  $\gamma$ . (b)  $N$  plotted against the strain  $\gamma$  at a fixed distance  $r$  between the particles. Legends:  $c$  denotes the concentration of vimentin in  $\text{mg mL}^{-1}$ ,  $R$  denotes the molar ratio of  $\text{Mg}^{2+}$  ions and vimentin monomers.

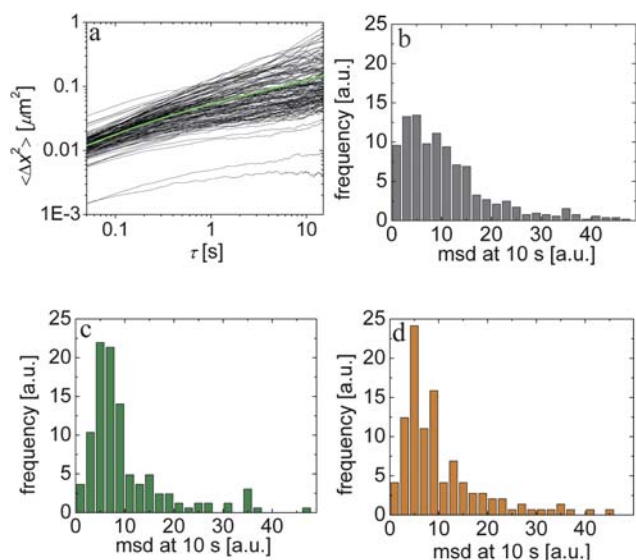


**Fig. 3** (a) Individual MSDs for microspheres in vimentin networks (shown here for 1  $\mu\text{m}$  microspheres in entangled network); (b–d) distribution of the MSD at 10 s for (b) microspheres in buffer, (c) microspheres in entangled vimentin network and (d) microspheres in cross-linked vimentin network.

In addition to analyzing the averaged MSDs we investigate the heterogeneity of the vimentin networks by studying the distribution of the MSDs of individual microspheres. A typical example is shown in Fig. 3a for 1  $\mu\text{m}$  diameter microspheres in an entangled network without added  $\text{Mg}^{2+}$ . The thick solid line shows the averaged MSD as plotted in Fig. 1c. We evaluate all sufficiently long MSDs for individual particles at a lag time of 10 s and normalize these values by the number of individual measurements and by the mean value at  $\tau = 10$  s, to allow us to compare the results. Histograms are shown in Fig. 3b for particles in buffer, in Fig. 3c for an entangled vimentin network and in Fig. 3d for a vimentin network cross-linked with the addition of 2 mM  $\text{Mg}^{2+}$ . The statistical spread in the data for particles in buffer is larger than that for particles in the vimentin networks. This implies that the network structure is rather homogeneous. Furthermore, the distributions of the MSDs in vimentin networks with and without  $\text{Mg}^{2+}$  are virtually the same, confirming that the addition of  $\text{Mg}^{2+}$  during assembly of vimentin into filaments and networks does not affect the assembly process itself, but instead only cross-links the network. This has also been confirmed by electron microscopy images (not shown).

Interestingly, cross-linked actin networks are rather homogeneous at relatively high values of  $R$  but become more heterogeneous as  $R$  is decreased.<sup>16</sup> The behavior of vimentin networks at even lower values of  $R$  has not yet been investigated.

## Experimental

Human vimentin protein is expressed in *Escherichia coli* (*E. coli*) bacteria and purified from inclusion bodies.<sup>17</sup> The protein is stored at  $-80$   $^{\circ}\text{C}$  in 8 M urea, 5 mM Tris–HCl (pH 7.5), 1 mM EDTA, 0.1 mM EGTA, 1 mM DTT, and 10 mM methyl ammonium chloride (MAC). The purity of the protein is verified by SDS-page electrophoresis. Before use in the experiments, the

protein is dialyzed, using membranes of 50 kDa cut-off, into 5 mM Tris (pH 8.4), 1 mM EDTA, 0.1 mM EGTA, and 1 mM DTT (dialysis buffer) in a stepwise manner (6, 4, and 2 M urea). The protein concentration is determined by a Bradford assay with bovine serum albumin (BSA) as a standard.

Microspheres (Invitrogen, Carlsbad, CA) with diameters 0.5, 1, and 2  $\mu\text{m}$  are coated with PLL(20)-g[3.5]-PEG(2) (SuSos, Zurich, Switzerland) to prevent adsorption of the IF proteins. We test the success of the coating of the microspheres by embedding them in assembled fibrin networks, which has a strong propensity for adsorption. Microspheres that are still motile are considered to be well coated. As an additional test, we add fluorescent BSA to the coated microspheres and verify that no protein adsorbs.

A drift-free sample chamber is assembled using microscope cover slips as bottom and top, with a silicone gasket spacer having a diameter of 9 mm and a depth of 0.5 mm (Invitrogen, Carlsbad, CA). The cell is sealed with high-viscosity vacuum grease. The protein solution is mixed with assembly buffer (10 $\times$  buffer: 200 mM Tris–HCl (pH 7.0) and 1.6 M NaCl), dialysis buffer, microspheres (0.5, 1, or 2  $\mu\text{m}$  diameter, Invitrogen), and, when needed,  $\text{MgCl}_2 \cdot 6\text{H}_2\text{O}$  to a final concentration of 1 mg mL<sup>-1</sup> vimentin, 1 $\times$  assembly buffer, and 2 mM  $\text{Mg}^{2+}$  ( $R = 105$ , when needed). The microsphere concentration is adjusted to ensure that they do not influence one another's motion. We pipette 40  $\mu\text{L}$  of this solution into the sample chamber, seal with vacuum grease, and place it on the microscope, where it is equilibrated for 1 h before the measurements are started. For each microsphere size, a control measurement in buffer with no protein present is performed prior to measurements in the protein networks.

For the non-affinity measurements under shear, vimentin networks at 3 and 4 mg mL<sup>-1</sup> are assembled in a similar manner.

Images (576  $\times$  576 pixels) are recorded with an inverted microscope (Leica, Wetzlar, Germany) equipped with a 40 $\times$  and a 63 $\times$  objective, both with long working distances. The frame rates are 1000 Hz and 20 Hz. We focus on the mid-plane of the sample chamber to avoid wall effects. Fluorescence images are recorded with a confocal microscope (Zeiss LSM 510, Jena, Germany) equipped with a 60 $\times$  water immersion objective at 488 nm laser excitation.

Data analysis is performed using IDL and Matlab code to track the individual microspheres and calculate the mean-squared displacements (MSDs) and the  $y(x)$  values. In brief, the images are inverted to obtain bright microspheres on a dark background and are band-passed to reduce pixel noise and long-wavelength image variations. The particle positions are determined first to pixel accuracy and then to sub-pixel accuracy. The MSDs of individual particles are calculated and then averaged. Care is taken to avoid drift in the data; in cases of obvious drift, the steady motion is removed in the analysis.

## Conclusions

We study the structure and mechanical properties of vimentin IF networks using microspheres of different diameters. We measure their thermal motion and calculate their average MSD. By using bead sizes smaller than the mesh size of the network, we probe the average mesh size. By using bead sizes larger than the mesh

size, we determine the network viscoelastic modulus. In addition, we subject the networks to an external shear strain and measure the degree of non-affinity of the deformation.

We find that the microspheres in the networks with no added  $Mg^{2+}$  continue to move, albeit with subdiffusive motion as compared to microspheres in buffer. When comparing MSDs of individual microspheres we observe some spread in the amplitudes but no change in the overall behavior for the individual microspheres. Similar to entangled actin networks, the subdiffusive motion may have its origin in jumping of the microspheres between adjacent microenvironments.

When  $Mg^{2+}$  is added, microspheres with a diameter  $\geq 1 \mu m$  are fully trapped. Addition of  $Mg^{2+}$  ions leads to cross-linking of vimentin networks,<sup>8</sup> consistent with these observations. By contrast, beads with a diameter of  $0.5 \mu m$  move subdiffusively similar to those in networks formed without  $Mg^{2+}$ . We use the motion of these beads, and the trapping of the larger beads to directly estimate the mesh size on the network. The mesh size so determined is  $\sim 1 \mu m$ , which is in reasonable agreement with estimates based on the concentration of vimentin assuming a cubic lattice model, and to estimates based on the elasticity of the network as determined from bulk rheology data.<sup>8</sup>

Interestingly, the cross-linking process does not change the structure of the network nor does the addition of divalent cations interfere with filament assembly and network formation. However, addition of  $Mg^{2+}$  at concentrations much lower than that needed for non-specific bundling by divalent cations leads to cross-linking of the vimentin networks in a manner similar to the cross-linking of actin networks by ABPs such as scruin or HMM.

## Acknowledgements

The IDL code used in this study was written by John Cocker, David Grier and Eric Weeks (for download see <http://www.physics.emory.edu/~weeks/idl/>). We would like to thank Norbert Mücke, Tatjana Wedig, Louise Jawerth, Karen Kasza,

Eliza Morris and Johannes Sutter for fruitful discussions and technical assistance. SK was supported by grants from the DFG, within the framework of the Excellence Initiative, the SFB 755 and KO 3572/1; HH was funded by DFG grants HE 1853. This work was supported by the NSF (DMR-0602684 and DBI-0649865), the Harvard MRSEC (DMR-0820484).

## Notes and references

- 1 H. Herrmann and U. Aebi, *Annu. Rev. Biochem.*, 2004, **73**, 749.
- 2 H. Herrmann, S. V. Strelkov, P. Burkhard and U. Aebi, *J. Clin. Invest.*, 2009, **119**, 1772.
- 3 C. Storm, J. J. Pastore, F. C. MacKintosh, T. C. Lubensky and P. A. Janmey, *Nature*, 2005, **435**, 191.
- 4 O. Lieleg, M. M. A. E. Claessens, C. Heussinger, E. Frey and A. R. Bausch, *Phys. Rev. Lett.*, 2007, **99**, 088102.
- 5 B. Schnurr, F. Gittes, F. C. MacKintosh and C. F. Schmidt, *Macromolecules*, 1997, **30**, 7781.
- 6 M. Schopferer, H. Bär, B. Hochstein, S. Sharma, N. Mücke, H. Herrmann and N. Willenbacher, *J. Mol. Biol.*, 2009, **388**, 133.
- 7 D. S. Fudge, K. H. Gardner, V. T. Forsyth, C. Riekel and J. M. Gosline, *Biophys. J.*, 2003, **85**, 2015.
- 8 Y.-C. Lin, N. Y. Yao, C. P. Broedersz, H. Herrmann, F. C. MacKintosh and D. A. Weitz, *Phys. Rev. Lett.*, 2010, **104**, 058101.
- 9 C. F. Schmidt, M. Baermann, G. Isenberg and E. Sackmann, *Macromolecules*, 1989, **22**, 3638.
- 10 I. Y. Wong, M. L. Gardel, D. R. Reichman, E. R. Weeks, M. T. Valentine, A. R. Bausch and D. A. Weitz, *Phys. Rev. Lett.*, 2004, **92**, 178101.
- 11 G. C. L. Wong, A. Lin, J.-X. Tang, Y. Li, P. A. Janmey and C. R. Safinya, *Phys. Rev. Lett.*, 2003, **91**, 018103.
- 12 M. Schopferer, H. Bär, B. Hochstein, S. Sharma, N. Mücke, H. Herrmann and N. Willenbacher, *J. Mol. Biol.*, 2009, **388**, 133.
- 13 M. L. Gardel, J. H. Shin, F. C. MacKintosh, L. Mahadevan, P. Matsudaira and D. A. Weitz, *Science*, 2004, **304**, 1301.
- 14 J. Liu, G. H. Koenderink, K. E. Kasza, F. C. MacKintosh and D. A. Weitz, *Phys. Rev. Lett.*, 2007, **98**, 198304.
- 15 D. A. Head, A. J. Levine and F. C. MacKintosh, *Phys. Rev. E: Stat., Nonlinear, Soft Matter Phys.*, 2003, **68**, 061907.
- 16 Y. Luan, O. Lieleg, B. Wagner and A. R. Bausch, *Biophys. J.*, 2008, **94**, 688.
- 17 H. Herrmann, I. Hoffmann and W. W. Franke, *J. Mol. Biol.*, 1992, **223**, 637.